Polish Journal of Microbiology
2016, Vol. 65, No 2, 225–229

SHORT COMMUNICATION

Cytotoxic and Bacteriostatic Activity of Nanostructured TiO_2 Coatings

ALESSANDRO DI CERBO[1]*, FEDERICA PEZZUTO[2] and ANTONIO SCARANO[3]

[1] School of Specialization in Clinical Biochemistry, University of Chieti-Pescara, Chieti, Italy
[2] Department of Clinical Microbiology, University of Modena and Reggio Emilia, Italy
[3] Department of Medical, Oral and Biotechnological Sciences, University of Chieti-Pescara, Chieti, Italy

Submitted 9 October 2015, revised and accepted 26 November 2015

Abstract

Nanostructures are structures, mainly synthetic (nanosurfaces, cylindrical nanotubes, and nanospheres), which range between 1–100 nm in at least one dimension and can be engineered to a wide range of physical properties. This paper aims to explore the bacteriostatic and cytotoxic characteristics of nano-TiO_2 coated specimens of glass, stainless steel and ceramic with different thickness and roughness. The results show that stainless steel and glass specimens with a nano-TiO_2 coating thickness of 200 nm have a bacteriostatic effect of 97% and 100%, respectively after 30 minutes of UV exposure. Glass specimens with a nano-TiO_2 coating thickness of 750, 200 and 50 nm have a bacteriostatic effect of 86%, 93% and 100% after 60 minutes. Nano-TiO_2 coatings show a great bacteriostatic but not a cytotoxic effect, thus representing a valuable alternative for biomedical applications.

Key words: bacteriostatic effect, cytotoxic activity, TiO_2 coatings

Bulk titanium oxide (TiO_2) does not exist in nature but is mainly derived from the industrial process of ilmenite (Tao *et al*., 2013). It is an n-type wide band-gap semiconductor with 3 crystalline phases, anatase, rutile and brookite, with rutile as the most stable form (Liao *et al*., 2012; Wang *et al*., 2014). Rutile and Anatase TiO_2 are widely used as photocatalysts although a mixed form of these two phases have displayed an enhanced photocatalytic ability (Kho *et al*., 2010; Li *et al*., 2008). Due to its high refractive index small amounts of TiO_2 can be used to achieve an opaque coating with a great resistance to discolor under UV light (Mikkelsen *et al*., 2011). In the last decade great interest arose from the field of synthesis and applications of nanostructured TiO_2 materials (Kulkarni *et al*., 2015). In this regard examples of applications are, for instance, dye-sensitized solar cells, sensors, rechargeable batteries, electrocatalysis, self-cleaning and antibacterial surfaces, photocatalytic cancer treatment and dental implants surface modification to prevent infections (Petrini *et al*., 2006; Seo *et al*., 2007; Roy *et al*., 2011; Cai *et al*., 2013; Lee *et al*., 2014; Behzadnia *et al*., 2014). An interesting application of TiO_2 is related to its use in coating different surfaces such as glass and tiles, providing them with deodorant, bactericidal (Pleskova *et al*., 2011; Yu *et al*., 2013) and self-cleaning (Xi *et al*., 2012; Khataee *et al*., 2013) activity once exposed to the UV light (Cai *et al*., 2013).

Based on such features it is also reasonable to hypothesize a possible use of this nanostructured material for biomedical applications such as operating rooms floor coatings, laboratory bench surface coating, as well as surgical instruments coating.

The aim of this study was to assess the bacteriostatic and cytotoxic activity of TiO_2 coatings on different bars made of glass, ceramic and stainless steel by means of a photocatalytic reaction following UV exposure. TiO_2 photocatalysis involves generation of hole (hþ) and electron (e) pairs and a subsequent reaction of surface-bound hydroxyl ions ($OH^{\cdot}$) and/or H_2O on TiO_2 particles with the holes to generate hydroxyl radicals ($OH^{\cdot}$) (Zuo *et al*., 2015).

TiO_2 coatings were performed by means of the electric arc physical vapour deposition (EA-PVD) technique (Kepenek *et al*., 2004) modified with the Electro Magnetic Controlled Arc Stirring (EMCAS). The first technique is characterized by a fast deposition rate, a good control of the process parameter in respect of conventional evaporation sources and the capability to coat very thin films of nanometric thickness (Giolli *et al*., 2007). As to the second technique, an electromagnetic device controls the electric arc movement

* Corresponding author: A. Di Cerbo, School of Specialization in Clinical Biochemistry, "G. d'Annunzio" University, Chieti, Italy; **e-mail: alessandro811@hotmail.it**

Table I
Physical features of sample used for the study

Code	Sample	Dimensions (mm)	Thickness (nm)	Roughness (μm)
AL	polished glass	6×50	200	0.08
AH	acid treated glass	6×50	200	0.3
AS	sandblasted glass	6×50	200	4.6
BL	polished glass	6×50	100	0.08
BH	acid treated glass	6×50	100	0.3
BS	sandblasted glass	6×50	100	4.6
CL	polished glass	6×50	50	0.08
CH	acid treated glass	6×50	50	0.3
CS	sandblasted glass	6×50	50	4.6
DL	polished glass	6×50	750	0.08
DH	acid treated glass	6×50	750	0.3
DS	sandblasted glass	6×50	750	4.6
EL	polished glass	6×50	750	0.08
EH	acid treated glass	6×50	750	0.3
ES	sandblasted glass	6×50	750	4.6
FL	polished glass	6×50	750	0.08
FH	acid treated glass	6×50	750	0.3
FS	sandblasted glass	6×50	750	4.6
ST	undeposited glass	6×50	–	–
ST	stainless steel	6×50	200	0.3
ST	ceramic tile	25×25	100	4.6

(scanning speed and position), the dimension of electric arc spot, and the time of permanence of spot in a desired position on the target so that it is possible to control the plasma density, the plasma temperature, the target wear and the evaporation zone of the target (Giolli *et al*., 2007). It is possible to distinguish two separate and different electric circuits of the deposition apparatus: 1) high voltage (up to 1000 V) and low current (< 5 A) for obtaining a plasma able to clean the substrates, and 2) relatively low voltages (5–30 V) and high currents (50–150 A) for coating the substrates; moreover, it is possible to apply to the substrates to be coated a negative bias.

All samples characteristics, provided by VACUUM SURTEC S.r.l., Parma, Italy, have been summarized in Table I.

Before any biological assay the surface of glass, ceramic and stainless steel specimens was previously observed and characterized by means of an environmental scanning electron microscope (ESEM, Quanta 200, Fei Company, Holland) and Energy Dispersive X-ray Analysis (EDS) for the presence of contaminants. Subsequently, samples were also analyzed by means of surface-conduction electron-emitter display (SED) and back-scattered electrons (BSE) analysis, at a low vacuum (0.98 Torr), 25–30 KV spectrum with different spots and at a distance of 10 mm (data not shown). Before each analysis each sample was sterilized in an autoclave at 120°C for 20 minutes.

***In-vitro* assays.** Specimen cytotoxicity was assessed according to the standard EN/ISO 10993/5 using Neutral Red (Sigma Aldrich St. Louis Missouri; USA) and 3-(4, 5-dimethylthiazolyl-2)-2, 5-diphenyltetrazolium bromide (MTT) (Life Technologies, Monza, Italy), whereas bacteriostatic activity was tested against *Staphylococcus aureus* by means of a Wood lamp (G.C.M., Milan, Italy) application at a 365 nm peak and at a distance of 10 cm which was previously recognized as safe in terms of bacterial death.

Each specimen was first rinsed with ethanol, then with acetone in a ultrasonic bath for 10 minutes and eventually accurately washed with deionized water for other 10 minutes. According to EN 30993-12 the ratio between sample area (> 1 mm) and the extraction liquid [(DULBECCO'S MEM, GIBCO™, UK) with Penicillin/Streptomycin (GIBCO™, UK) 100 IU/100 μg/ml, 2 mM L-glutamine, 1 mM Sodium Pyruvate and 10% fetal calf serum (Euroclone, Milan, Italy)] was: A/V = 3 cm^2/ml. Each sample was then incubated at 37°C with 5% CO_2.

As to Neutral Red and MTT assay we used murine fibroblasts L929 at a concentration of 5×10^4 and 10×10^3 and uniformly distributed in 6 and 96 MW in 3 and 0.2 ml of MEM, respectively.

Copper was used as a positive control for both assays whereas a cell culture without specimen was used as a negative control.

Microscopic evaluations were performed by means of an optical microscope (Nikon Eclipse E600 microscope, Japan) whereas spectrophotometric analyses of wells were performed by a HP 8452 diode array spectrophotometer (St. Paul. GMI Inc. USA) at 540 nm.

As to cytotoxic evaluations, 100 mm plastic petri dishes (Life Technologies, Monza, Italy) were used to place both specimen and 3 ml (4 ml only for ceramic specimen) of a 5 mM saline solution which was achieved from 3 serial dilutions of a 0.5 M solution with *Staphylococcus aureus* ATCC 6538. Serial dilutions were used to allow the operator to easily count the remaining colonies following UV light exposure. Then, before starting the UV light exposure (time 0), after 30 minutes of exposure (time 30) and after 60 minutes of exposure (time 60) 10 μl of solution was withdrawn from the petri dish and placed onto a blood Agar (TSA with 5% Sheep Blood)/MacConkey plate (Life Technologies, Monza, Italy).

Statistical analysis. Data were analyzed using GraphPad Prism 6 software (GraphPad Software, Inc., La Jolla, CA, USA). All data are presented as the means ± standard error of the mean and were first checked for normality using the D'Agostino-Pearson normality test. Differences between samples were analyzed using Friedman Test with Dunn's multiple comparisons test. $p < 0.05$ was considered significant.

Neutral Red assay. Neutral Red assay highlighted a great viability and numerosity of cells in contact with AL, AS and AH as well as clearly colored as for the negative control (data not shown). Conversely, cell numerosity resulted quite reduced for BH, BL and BS specimens, less stained and rod shaped meaning a suffering condition which was the same of that observed for the negative control (data not shown).

MTT assay. MTT assay on TiO_2-coated polished and sandblasted glass clearly indicated that cell proliferation was quite the same as for negative control, thus meaning the lack of any cytotoxic activity (Fig. 1).

Microbiological assay. Before each experiment stainless steel, glass and ceramic specimens were first placed in respective petri dishes along with a 5 mM saline solution with *S. aureus* ATCC 6538, as previously described in the materials and methods section. Then before starting the UV light exposure (time 0), at a 10 cm distance, after 30 minutes of exposure (time 30) and after 60 minutes of exposure (time 60) 10 µl of solution were withdrawn from the petri dish and placed in triplicate into blood Agar/MacConkey plates. Then, all plates of all specimens were placed at 37°C overnight and a mean of all colonies for each specimen was determined.

Firstly, a comparative analysis of ceramic, stainless steel and glass (AL) was performed to better evaluate differences, in terms of bacteriostatic activity, between different specimens (Fig. 2A).

Figure 2A clearly shows a marked bacteriostatic effect of stainless steel and glass specimens (97% and 100%, respectively), with respect to the positive control, already after 30 minutes of UV light exposure, thus highlighting the possible enhanced bacteriostatic activity of TiO_2-coating. On the contrary, the ceramic specimen seemed to share the same trend of positive control, thus evidencing the absence of a possible bacteriostatic activity induced by TiO_2-coating. As to negative control, it showed the normal trend of *S. aureus* ATCC 6538 which had not been exposed to UV light, thus confirming the bacteriostatic activity of all specimens.

Based on these result the bacteriostatic activity on glass specimens was evaluated with different TiO_2-coating thickness in order to observe any differences in terms of bacterial growth inhibition (Fig. 2B).

A marked bacteriostatic effect of glass specimens AL, CL, and FS, was observed with respect to the positive control, as well as an overall decrease of *S. aureus* ATCC 6538 colonies of 100%, 93%, and 86% respectively after 60 minutes of UV light exposure, thus highlighting the possible enhanced bacteriostatic activity of TiO_2-coating. DS specimen showed a good bacteriostatic effect with a decrease of *S. aureus* ATCC 6538 colonies of 66% after 60 minutes of UV light exposure.

As for BH and EH specimens, a poor bacteriostatic activity was observed since there was only a 49% and

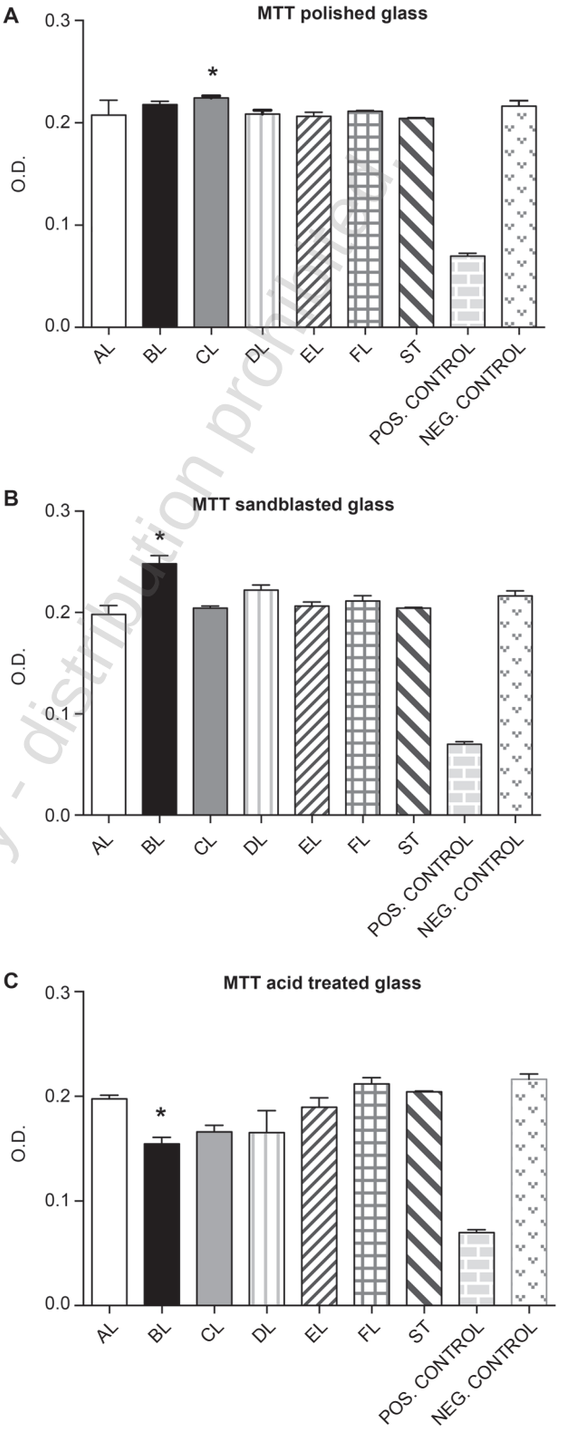

Fig. 1. Graphical representation of cytotoxic activity of TiO_2-coated glass with different treatments. (A) polished, (B) sandblasted, (C) acid treated; (*$p < 0.05$).

56% decrease of S. aureus ATCC 6538 colonies after 60 minutes of UV light exposure.

This study aimed to evaluate the response of stainless steel, glass and ceramic specimens with TiO_2 layers

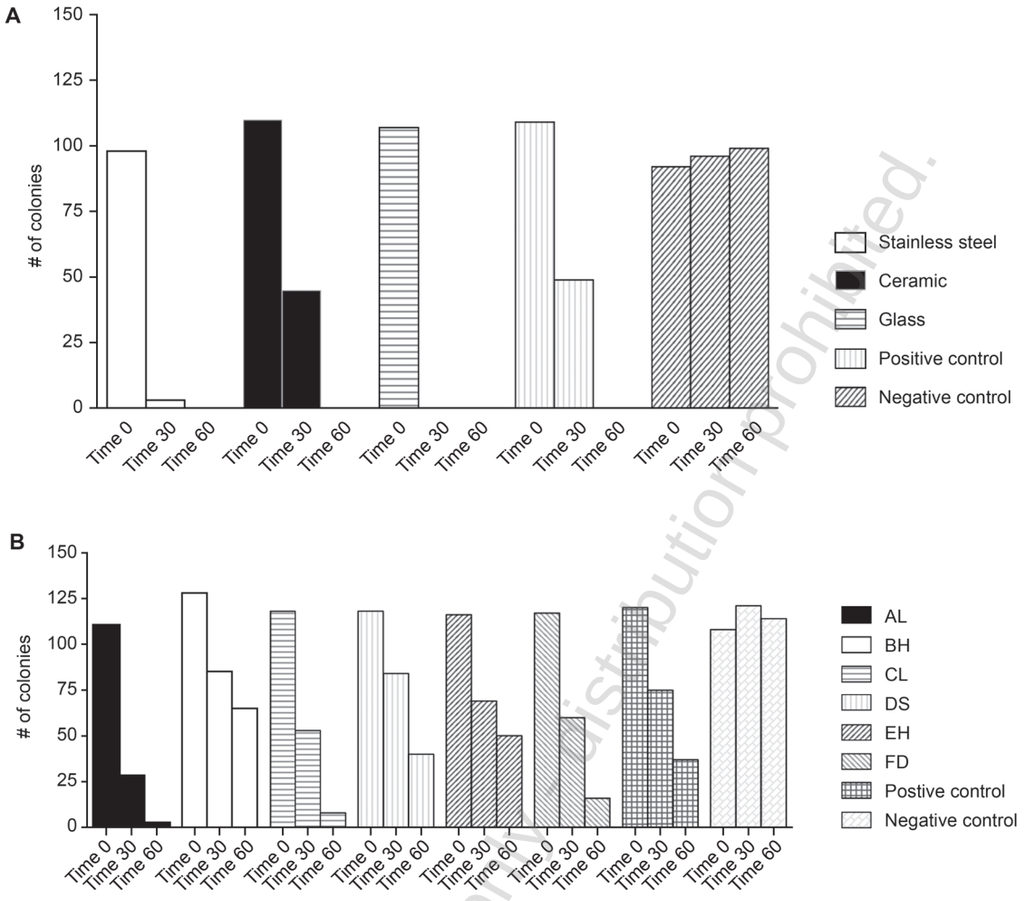

Fig. 2. Graphical representation of *S. aureus* ATCC 6538 colonies trend during the study.

(A) Before starting the UV light exposure (time 0), after 30 minutes of exposure (time 30) and after 60 minutes of exposure (time 60). The positive control was *S. aureus* ATCC 6538 exposed to UV light, while the negative control was the same strain but not exposed to UV light; (B) Before starting the UV light exposure (time 0), after 30 minutes of exposure (time 30) and after 60 minutes of exposure (time 60) on glass specimens with different TiO_2-coating thickness. The positive control was the *S. aureus* ATCC 6538 exposed to UV light, while the negative control was the same strain but unexposed to UV light.

of different thickness coated by means of the electric arc physical vapour deposition technique. Neutral Red assay pointed out that BL, BH and BS specimens showed a marked reduction of bacterial proliferation with respect to positive control while AL, AH and AS specimens only showed a slight reduction. Conversely, the MTT assay evidenced the almost lack of cytotoxicity of the specimens. This is in agreement with previous literature reports which showed the biocompatibility of TiO_2 so that it is commonly used for different biomedical applications (He *et al.,* 2013; Kulkarni *et al*., 2015).

We hypothesized that the lack of a cytotoxic effect was either due to a partial penetration of UV light which was unable to trigger the photocatalytic effect or due some surface structure alterations. As to bacteriostatic effects, these resulted particularly enhanced with AL, EH, CL and FS glass specimens.

In conclusion, this study revealed that both the bacteriostatic and cytotoxic effects depended on the kind of material and on its TiO_2 thickness. Thus, further experiments are required to overcome the lack of information about nanostructured surfaces for future biomedical applications.

Literature

Behzadnia A., M. Montazer and A. Rashidi. 2014. Rapid sonosynthesis of N-doped nano TiO2 on wool fabric at low temperature: introducing self-cleaning, hydrophilicity, antibacterial/antifungal properties with low alkali solubility, yellowness and cytotoxicity. *Photochem Photobiol.* 90: 1224–1233.

Cai Y., M. Stromme and K. Welch. 2013. Photocatalytic antibacterial effects are maintained on resin-based TiO2 nanocomposites after cessation of UV irradiation. *PLoS One* 8: e75929.

European Patent Application (EPA). EP 1 624 087 A1.

Giolli C., F. Borgioli, A. Credi, A. Di Fabio, A. Fossati, M. Muniz Miranda, S. Parmeggiani, G. Rizzi, A. Scrivani, S. Troglio and others. 2007. Characterization of TiO2 coatings prepared by a modified electric arc-physical vapour deposition system. *Surface & Coatings Technology* 202: 13–22.

He R., L. Zhao, Y. Liu, N. Zhang, B. Cheng, Z. He, B. Cai, S. Li, W. Liu, S. Guo and others. 2013. Biocompatible TiO2 nanoparticle-based cell immunoassay for circulating tumor cells capture and identification from cancer patients. *Biomed. Microdevices* 15: 617–626.
Kepenek, B., U.O.S. Seker and A.F. Cakir. 2004. Photocatalalytic bactericidal effect of TiO2 thin film produced by Cathodic Arc Deposition Method. *Key Engineering Materials* 254–256: 463–466.
Khataee R., V. Heydari and L. Moradkhannejhad. 2013. Self-cleaning and mechanical properties of modified white cement with nanostructured TiO2. *J. Nanosci. Nanotechnol.* 13: 5109–51014.
Kho Y.K., A. Iwase and W.Y. Teoh. 2010. Photocatalytic H2 evolution over TiO2 nanoparticles. The synergistic effect of anatase and rutile. *J. Phys. Chem. C.* 114: 2821–2829.
Kulkarni M., A. Mazare and E. Gongadze. 2015. Titanium nanostructures for biomedical applications. *Nanotechnology* 26: 062002.
Lee K., A. Mazare and P. Schmuki. 2014. One-dimensional titanium dioxide nanomaterials: nanotubes. *Chem. Rev.* 114: 9385–9454.
Li G., N.M. Dimitrijevic and L. Chen. 2008. The important role of tetrahedral Ti4+ sites in the phase transformation and photocatalytic activity of TiO2 nanocomposites. *J. Am. Chem. Soc.* 130: 5402–5403.
Liao Y., W. Que and Q. Jia. 2012. Controllable synthesis of brookite/anatase/rutile TiO2 nanocomposites and single-crystalline rutile nanorods array. *J. Mater. Chem.* 22: 7937–7944.
Mikkelsen L., M. Sheykhzade and K.A. Jensen. 2011. Modest effect on plaque progression and vasodilatory function in atherosclerosis-prone mice exposed to nanosized TiO(2). *Part Fibre Toxicol.* 8: 32.
Petrini P., C.R. Arciola and I. Pezzali. 2006. Antibacterial activity of zinc modified titanium oxide surface. *Int. J. Artif. Organs* 29: 434–442.
Pleskova S.N., I.S. Golubeva and I. Verevkin. 2011. Photoinduced bactericidal activity of TiO2 films. *Prikl. Biokhim. Mikrobiol.* 47: 28–32.
Roy P., S. Berger and P. Schmuki. 2011. TiO2 nanotubes: synthesis and applications. *Angew. Chem. Int. Ed. Engl.* 50: 2904–2939.
Seo J.W., H. Chung and M.Y. Kim. 2007. Development of water-soluble single-crystalline TiO2 nanoparticles for photocatalytic cancer-cell treatment. *Small* 3: 850–853.
Tao T., Y. Chen and D. Zhou. 2013. Expanding the applications of the ilmenite mineral to the preparation of nanostructures: TiO2 nanorods and their photocatalytic properties in the degradation of oxalic acid. *Chemistry* 19: 1091–1096.
Wang Y., Y. He. and Q. Lai. 2014. Review of the progress in preparing nano TiO2: an important environmental engineering material. *J. Environ. Sci.* (*China*) 26: 2139–2177.
Xi B., L.K. Verma and J. Li. 2012. TiO2 thin films prepared via adsorptive self-assembly for self-cleaning applications. *ACS Appl. Mater. Interfaces.* 4: 1093–10102.
Yu B., W. M. Lau and J. Yang. 2013. Preparation and characterization of N-TiO2 photocatalyst with high crystallinity and enhanced photocatalytic inactivation of bacteria. *Nanotechnology* 24: 335705.
Zuo X., J. Hu. and M. Chen. 2015. The role and fate of inorganic nitrogen species during UVA/TiO disinfection. *Water Res.* 80: 12–19.